Sensor applications

Investigation of Thermal Anemometry With Thermistor Sensing Elements for Gas Flow Measurements in Harsh Environments

Martin Schellander, Bernhard Schweighofer, Markus Neumayer*, and Hannes Wegleiter

Christian Doppler Laboratory for Measurement Systems for Harsh Operating Conditions, Institute of Electrical Measurement and Sensor Systems, Graz University of Technology, 8010 Graz, Austria

Member, IEEE

Manuscript received 19 June 2023; revised 27 July 2023; accepted 1 August 2023. Date of publication 7 August 2023; date of current version 23 August 2023.

Abstract—The production of high-quality steel requires purging with argon to remove impurities, degas the molten metal, and optimize the alloying process. However, sealing challenges in steelworks result in variable argon losses. But accurate mass flow measurements are crucial for process optimization. This letter investigates the feasibility of a ladle-based argon flow sensor system to overcome these challenges. The system must address high gas velocities, wide fluid temperature range, and limited power availability. The study focuses on a thermal anemometer with thermistors as sensing elements, evaluating sensitivity, cross-sensitivity, and power consumption on a test rig.

Index Terms—Sensor applications, flow rate measurement, harsh environment, low power, thermal anemometry.

I. INTRODUCTION

The purging process with inert gases, particularly argon, plays a crucial role in steel production [1]. It is carried out through bottom blowing of liquefied metal with argon, which involves the use of a porous purge plug [2]. The amount of purging gas being used is crucial for the quality of the steel and the productivity of the process [3], [4].

This process occurs within steel ladles, which transport liquid steel between production stages, as shown in Fig. 1. However, achieving a secure and durable seal for the gas injection line on the ladles, subjected to extreme conditions, proves challenging, leading to unknown argon leakage. Hence, a reliable and accurate flow sensing system capable of withstanding harsh conditions (in particular, the large temperature variations—the gas temperature ranges from 0 °C to up about 150 °C—and possible contamination of the gas stream with small particles due to the dusty environment) and providing direct flow rate measurements within the argon pipe is required. Furthermore, due to the lack of the possibility to use wired connections from the ladle to some external power supply, the measurement system has to be energy self-sufficient. This significantly limits the maximum available sensor power.

In the industry, various flow measurement techniques are employed, each with specific advantages and limitations [5], [6]. Thermal anemometry, particularly hot wire anemometry, stands out as a promising method due to its direct sensitivity to mass flow, suitability for large flow rate ranges [7], and, depending on the design of the sensing element, high mechanical robustness and low power consumption.

In a previous work [8], we have already shown that by using a negative temperature coefficient (NTC)-thermistor -based thermal anemometer, we can most probably satisfy the requirements on the measuring system. However, the test rig at that time was very limited (gas velocity limited to about 16 m/s, which is only a third of the required velocity, only minimal heating capability—about 20 °C, and no way to simulate back pressure as it occurs in the application), so that only a partial statement could be made with respect to the flow rate, but not really with respect to temperature influence and backpressure. Within the scope of this work we have solved this problem—the test stand is now able to reproduce the complete working range as it occurs in reality on the ladle (see also Table 1). We also reduced the thermal coupling of the thermistor with the printed circuit board (PCB), which significantly improved the behavior of the measurement system (see also Fig. 2).

The rest of this letter is organized as follows. In Section II, we will shortly review thermal anemometry, and the design of the sensor and its model. Section III presents the test rig that is used to characterize the sensor. Finally, in Section IV, we will present the characterization of the sensor.

II. SENSOR CONCEPT

A. Thermal Anemometry

Thermal anemometry offers several advantages, such as high sensitivity at low flow rates, a wide range of measurable flow rates, and the ability to design a robust and durable sensor that can withstand harsh environments [9], [10], [11]. Moreover, the conclusions derived from the study conducted by Benincasa et al. [8] emphasize that thermal anemometers employing thermistor-based sensing elements exhibit high sensitivity to flow rate while consuming low power. This characteristic makes them highly suitable for systems operating under energy constraints, especially using the constant overtemperature mode.

B. Sensor Design

Thermistors as sensing elements present a sensor design that is robust, offering advantages in terms of sensor dynamics and expected power consumption [8]. They are available in compact sizes and can operate effectively across a wide range of temperatures.

The two needed thermistors are placed next to each other, as described in [12]. However, it is important to note that a larger distance (longer wires) between the thermistors and the circuit board

Corresponding author: Bernhard Schweighofer (e-mail: bernhard.schweighofer@tugraz.at).

Associate Editor: B. Jakoby.

Digital Object Identifier 10.1109/LSENS.2023.3303069

leads to better results. This can be explained by the lower thermal coupling via the (longer) connecting wires of the thermistors to the PCB. On one hand, this thermal coupling transfers power from the heated thermistor to the PCB, which increases the power required to reach the desired overtemperature of the (sensing) thermistor. At the same time, this heat flow heats the PCB, which affects the transferred power—so the transferred power is not constant, but changes over time. In the experiment, time constants in the minute range were found for the transient process until steady-state conditions were established. On the other hand, the changed PCB temperature also has an influence on the second thermistor, which should actually only be sensitive to the gas temperature. The used design for the test bench (with long connection wires) is shown in Fig. 2 to the right.

In the constant overtemperature mode, one of the two thermistors is heated to a given overtemperature in comparison to the fluid temperature measured by the second thermistor [13]. The power necessary to maintain this overtemperature is the measurement value, which enables the calculation of the flow rate of the medium [14].

C. Sensor Model

Due to the wide operating range of flow rates, it is not possible to express the behavior in a single analytical equation [15], [16]. To overcome this challenge, Bruun [17] suggested dividing the flow rate range into two subranges.

1) *Lower flow rate range of* $< 6.6\,\frac{Nm^3}{h}$*:* In this range, natural heat convection is strong enough to affect forced heat convection, and therefore, it is described as the mixed convection regime.
2) *Upper flow rate range of* $> 6.6\,\frac{Nm^3}{h}$*:* In this range, the forced heat convection dominates.

The physical meaning of an according sensor model is derived in [17] and [18] for the upper flow rate range. This derivation leads to an equation of the form

$$P_{\mathrm{NTC}} = A + B \cdot q_{V,N}^{C} \tag{1}$$

with the normal volumetric flow rate $q_{V,N}$, the convection power P_{NTC} that is needed to keep the sensing NTC-thermistor at a constant overtemperature, and the three optimization parameters A, B and C. The optimization variables are found by calibration with experimental data. For the lower flow rate range, no derivation of an analytical equation could be found in literature. Therefore, a model has to be found by experimentation.

D. Power Limitations

Self-sufficiency is crucial for the given application. Therefore, the system relies on a thermoelectric generator, which must generate enough energy for the measurement system. An energy storage system is needed to supply the system during times with low power generation. Tests in the field have shown that using a standard 40×40 mm^2 Peltier element, a mean power production of about 150 mW is possible. By considering the individual consumers, such as microcontrollers and radio communication components, as well as the time required for the purging process, maximum power available for the thermal anemometer can be estimated to be approximately 350 mW.

III. TEST RIG

In order to assess the performance of a thermal anemometer in a steel production environment, a well-designed test rig is essential.

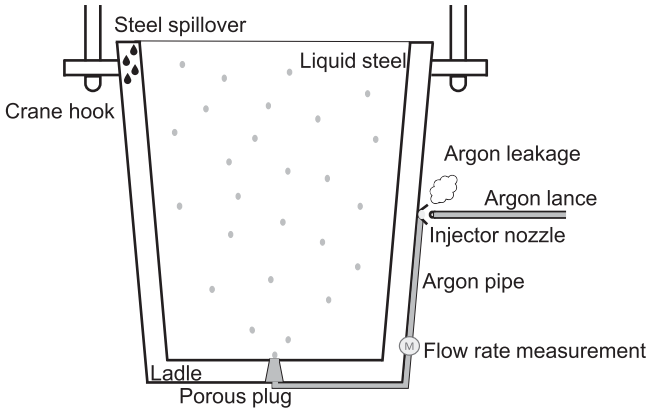

Fig. 1. Steel ladle during the argon purging process.

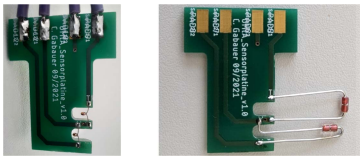

Fig. 2. Pictures of the sensor design (fluid direction from left to right). Left—design used in [8]. Right—"improved" design with longer connection wires (used in this work).

Table 1. Operating conditions in the steel purging process

Quantity	Operating range
Temperature of the argon gas	0 ... 150 °C
Pressure within the pipe	≈ 3 bar, short spikes up to 10 bar
Volumetric flow rate	6 ... 42 N.m^3/h
Gas velocity	5 ... 50 m/s

This test rig accurately replicates the operating conditions outlined in Table 1, enabling to thoroughly evaluate the behavior and accuracy of the anemometer under specific process conditions. Fig. 3 illustrates the incorporation of various sensors, control systems, and components for this purpose.

By utilizing the test rig, the anemometer's ability to precisely measure flow rates across a wide range of temperatures and flow rates can be verified. To simulate ladle conditions, the test rig utilizes pressurized air and a heating control system. To determine the sensor's behavior, a commercially available flow rate sensor (Höntzsch[1]: Thermal measuring tube TA Di with an internal diameter of 21.6 mm and integrated transducer U10b; the measurement uncertainty is about 2% over the considered working range.) is positioned in front of the heater, providing reference measurements.

The characterization of the sensor with air using the test bed provides a reliable baseline for comprehending the sensor's behavior with argon. Through the study of the sensor's performance and response characteristics in air, valuable insights can be gained into its expected behavior and performance when exposed to argon gas. However, it is important to note that for real-world applications in the argon purging process, a calibration using argon should be performed to ensure accurate and precise measurements.

[1][Online]. Available: www.hoentzsch.com

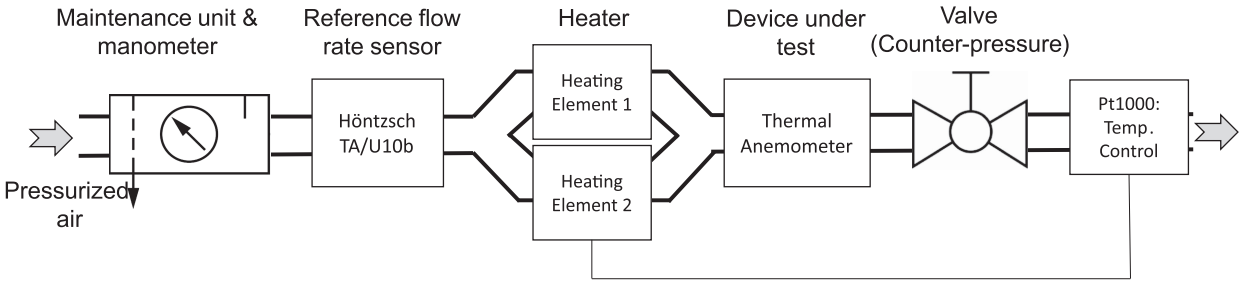

Fig. 3. Components of the test rig to replicate real-world conditions and characterize the proposed sensor design.

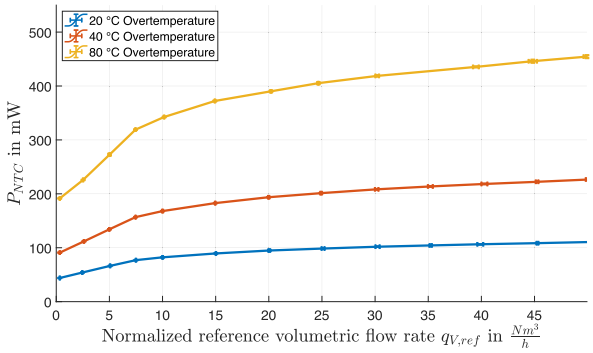

Fig. 4. Required power P_{NTC} to maintain the given overtemperature as a function of flow rate $q_{V,\mathrm{ref}}$. The pressurized air had a temperature of about 23 °C. The error bars denote three times the standard deviation ($\pm 3 \cdot \sigma$).

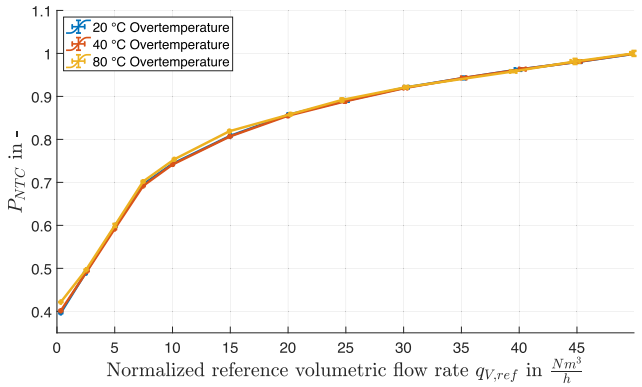

Fig. 5. Normalized sensor power P_{NTC} to maintain the given overtemperature as a function of flow rate $q_{V,\mathrm{ref}}$. The pressurized air had a temperature of about 23 °C. The error bars denote three times the standard deviation ($\pm 3 \cdot \sigma$).

IV. SENSOR CHARACTERIZATION

A. Methodology

Measurements for varying flow rates, temperatures, and pressures utilizing the test rig were conducted. For each measurement point, a snapshot of 100 measurement values were taken, requiring approximately 5 s to complete ($T_{\mathrm{sample}} \approx 50\,\mathrm{ms}$). From these samples, the mean value and standard deviation are calculated and represented in an error bar plot.

B. Different Overtemperatures

In the first experiment, the behavior of the sensing power for different flow rates was investigated. Therefore, the flow rate was varied over the whole operating range, while measuring the sensor power. The results for overtemperatures of 20 °C, 40 °C, and 80 °C are shown in Fig. 4.

In order to assess the sensitivity of the sensor at different overtemperatures, the measured power was normalized to the highest power measured for each corresponding overtemperature. The results of the normalization have shown that the sensitivity of the measurement does not change with different overtemperatures, as shown in Fig. 5.

For the upcoming sections, an overtemperature of 40 °C has been selected based on several factors. First, this setting provides a promising SNR, which is critical for accurate measurements. In addition, this overtemperature is still within the allowed power range given by the energy harvester (see Section II-D).

C. Sensor Model

The result of the sensor model fit for both flow rate ranges is shown in Fig. 6. For the lower flow rate regime, a linear model was used,

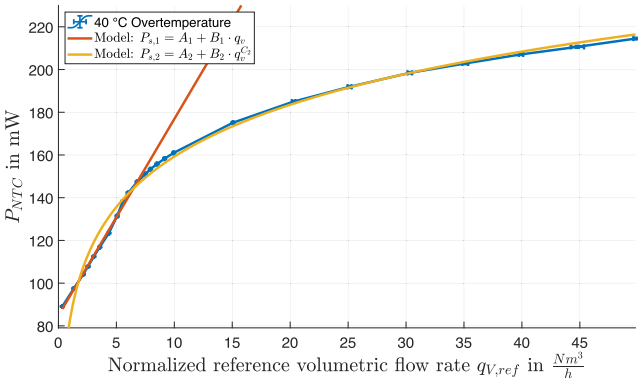

Fig. 6. Sensor model compared to the measurements at an overtemperature of 40 °C. The error bars denote three times the standard deviation ($\pm 3 \cdot \sigma$).

whereas for the higher flow rate regime, the proposed form from (1) was used.

The sensor model and the measurements agree well with each other in both flow rate ranges. In addition, the transition of the flow rate subregimes match the prediction in [17].

D. Cross-Sensitivity

To analyze the influence of varying fluid temperatures or counterpressures on the measurement result, a cross-sensitivity analysis was conducted. The variation of the fluid temperature leads to a change of the thermal properties of the fluid. This effect makes a variation of the

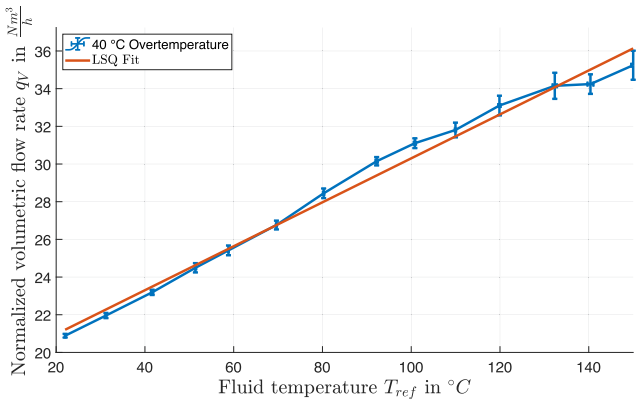

Fig. 7. Cross-sensitivity to fluid temperature change for a flow rate of 20 $\frac{\mathrm{N\,m^3}}{h}$ and a constant overtemperature of 40 °C. The error bars denote three times the standard deviation ($\pm 3 \cdot \sigma$).

heating power depending on the fluid temperature very likely [19]. For that purpose, the flow rate was set to a constant value of 20 $\frac{\mathrm{N{\cdot}m^3}}{h}$. The temperature of the air was then varied across a temperature range of 25 °C–150 °C. Fig. 7 shows the result of the flow rate measurement for different fluid temperatures. To calculate the flow rates from the power measurements, the model shown in the previous Section IV-C was used.

The influence of the temperature is significantly and has to be taken into account when measuring the flow rate of fluids with varying temperatures. However, as shown in Fig. 7, a simple linear model is sufficient to compensate for this effect.

The cross-sensitivity of the flow rate measurements to counter-pressure in the pipe was also investigated. However, varying the back pressure in the range of 0–8 bar did not show any (measurable) effect on the flow rate predicted by the sensor.

V. CONCLUSION

This letter introduces a thermal anemometry-based sensor system designed for measuring flow rates during the argon purging process in steel production. The sensor utilizes thermistors as sensing elements and offers robustness, high sensitivity across a wide temperature range, and accurate flow rate measurements. The study includes a sensor model that combines an analytical equation and experimental data to accurately measure flow rates. Furthermore, this letter describes a test rig that simulates real-world conditions and validates the sensor's performance. Results indicate the sensor's sensitivity to flow rates, a linear fluid temperature cross-sensitivity, and negligible cross-sensitivity to counter-pressure. Overall, this research presents a reliable and accurate flow rate sensing solution for the use in steel purging.

ACKNOWLEDGMENT

This work was supported in part by the Austrian Federal Ministry for Digital and Economic Affairs, in part by the National Foundation for Research, Technology and Development, Austria, in part by the Christian Doppler Research Association, in part by the voestalpine Stahl Donawitz GmbH, and in part by the TU Graz Open Access Publishing Fund, Austria.

REFERENCES

[1] V. Zeljkovic, P. Praks, and I. Husar, "Monitoring the impact of the intensity of blowing of an inert gas to the visual character of the molten steel surface," in *Proc. IEEE Int. Energy Conf.*, 2010, pp. 385–388.
[2] M. Nag, T. Agrawal, B. Nag, B. Singh, and S. Biswas, "Study and post mortem analysis of steel ladle porous plug to improve bottom purging efficiency for cleaner steel," *Eng. Failure Anal.*, vol. 101, pp. 447–455, 2019.
[3] A. L. V. da C. e Silva, "Non-metallic inclusions in steels-origin and control," *J. Mater. Res.*, vol. 7, no. 3, pp. 283–299, Jul.–Sep. 2018.
[4] A. Ghosh, *Secondary Steelmaking*. Boca Raton, FL, USA: CRC, 2000.
[5] K. D. Jensen, "Flow measurements," *J. Braz. Soc. Mech. Sci. Eng.*, vol. 26, no. 4, pp. 400–419, 2004.
[6] R. C. Baker, *Flow measurement handbook*. New York, NY, USA: Cambridge Univ. Press, 2016.
[7] D. W. Spitzer, *Flow Measurement: Practical Guides for Measurement and Control*. Triangle Park, NC, USA:Instrum. Soc. Amer., 1991.
[8] G. Benincasa et al., "Lab investigation of thermal anemometers for mass flow measurements in harsh operating conditions," in *Proc. IEEE Int. Instrum. Meas. Technol. Conf.*, 2022, pp. 1–6.
[9] R. Montgomery and R. McDowall, *Fundamentals of HVAC Control Systems*. Atlanta, GA, USA: Amer. Soc. Heating, Refrigerating Air-Conditioning Eng., Inc., 2010.
[10] A. Bekraoui and A. Hadjadj, "An overview of thermal mass flowmeters applicability in oil and gas industry," *Energy Procedia*, vol. 141, pp. 299–303, 2017.
[11] J. O. Bird and P. J. Chivers, "Measurement of fluid flow," in *Newnes Engineering and Physical Science Pocket Book*. Oxford, U.K.: Newnes, 1993, pp. 370–381.
[12] H. Fujita, T. Ohhashi, M. Asakura, M. Yamada, and K. Watanabe, "A thermistor anemometer for low-flow-rate measurements," *IEEE Trans. Instrum. Meas.*, vol. 44, no. 3, pp. 779–782, Jun. 1995.
[13] R. F. A. Assis, S. Y. C. Catunda, D. R. Belfort, and I. Muller, *Energy Performance of NTC-Based Constant Temperature Anemometers*. 2017, pp. 1–6.
[14] G. P. Russo, "Hot wire anemometer," in *Aerodynamic Measurements*. New Delhi, India: Woodhead, 2011, pp. 67–98.
[15] M. K. Swaminathan, G. W. Rankin, and K. Sridhar, "A note on the response equations for hot-wire anemometry," *J. Fluids Eng.*, 1986.
[16] H. H. Bruun, M. A. Khan, H. H. Al-Kayiem, and A. A. Fardad, "Velocity calibration relationships for hot-wire anemometry," *J. Phys. E: Sci. Instrum.*, vol. 21, 1988, Art. no. 225.
[17] H. H. Bruun, *Hot-Wire Anemometry: Principles and Signal Analysis*. Bristol, U.K.: IOP, 1996.
[18] A. E. Perry, *Hot-Wire Anemometry*. London, U.K.: Oxford Univ. Press, 1982.
[19] B. E. Poling, J. M. Prausnitz, and J. P. Connell, *The Properties of Gases and Liquids*. New York, NY, USA: McGraw-Hill, 2001.